

# Origin of Interplanetary Southward Magnetic Fields Responsible for Major Magnetic Storms Near Solar Maximum (1978-1979)

BRUCE T. TSURUTANI,<sup>1</sup> WALTER D. GONZALEZ,<sup>1,2</sup> FRANCES TANG,<sup>3</sup> SYUN I. AKASOFU,<sup>4</sup> AND EDWARD J. SMITH<sup>1</sup>

The origins of the interplanetary southward  $B_z$  which cause the 10 major ( $D_{st} < -100$  nT) magnetic storms detected during the 500 days of study (August 16, 1978, to December 28, 1979) of the Gonzalez and Tsurutani (1987) work are examined in detail. A full complement of ISEE 3 plasma and field data, an 11-station  $AE$  index and the near-equatorial  $D_{st}$  index, are used in this analysis. It is found that the origins of the interplanetary southward  $B_z$  events are quite varied. If it is defined that the  $B_z$  event which leads to  $D_{st} < -100$  nT is "the cause" of the storm, then one of the storm intensifications is caused by shock compression of preexisting southward interplanetary magnetic fields, four (or five) are related to driver gas magnetic fields, one (or two) are caused by shocked kinky heliospheric current sheets, two (or three) by turbulence or waves behind interplanetary shocks, and one possibly by draped fields associated with a noncompressive density enhancement event (without a shock or a high-speed stream). In simplistic terms, four (or five) storms are caused by driver gas fields, four by shocked (sheath) fields, and one possibly by high-intensity draped fields. In actuality, many of the interplanetary southward  $B_z$  and corresponding magnetic storm ( $D_{st}$ ) structures are more complex than stated above. At least four of the interplanetary events have both major sheath and driver gas southward  $B_z$  events. In two storms, sheath southward  $B_z$  features led to  $D_{st}$  reaching levels of  $-90$  nT prior to driver gas southward  $B_z$  features; the following driver gas fields then caused  $D_{st}$  to exceed our storm criteria of  $\leq -100$  nT. In two other cases, sheath  $B_z$  features led to magnetic storm onsets ( $D_{st} < -100$  nT); the following driver gas southward  $B_z$  features cause further storm intensifications. The above magnetic storms therefore displayed two-stage development characteristics. The results of this study indicate the equal importance of both sheath fields or draped fields and driver gas fields for the generation of major geomagnetic storms. Because of the importance of the sheath fields the intensity and duration of geomagnetic storms cannot be predicted by solar observations of active regions alone. Tang et al. (1988) will address this topic in detail.

## INTRODUCTION

To be able to eventually forecast impending geomagnetic storms at the earth in a quantitative fashion, the causes of responsible interplanetary events and their solar origins must be thoroughly understood. The first step of this important link (working from Earth backward) is well established. Intense southward interplanetary magnetic fields (IMFs) are well documented as causing magnetic storms [Rostoker and Fälthammar, 1967; Hirshberg and Colburn, 1969; Patel and Wiskerchen, 1975; Burton et al., 1975; Akasofu et al., 1985; Murayama, 1986; Smith et al., 1986; Zwickl et al., 1987; Gonzalez and Tsurutani, 1987] presumably through the process of magnetic reconnection [Dungey, 1961]. Gonzalez and Tsurutani [1987] have demonstrated that interplanetary events with dawn-dusk  $E > 5$  mV/m (approximately IMF  $B_z \leq -10$  nT) and with  $\tau > 3$  hours have a one-to-one causal relationship with intense ( $D_{st} < -100$  nT) magnetic storms. They established that 9 out of 10  $B_z$  events followed interplanetary shocks within 36 hours; the tenth event was a noncompressive density enhancement event [Belcher and Davis, 1971; Gosling et al., 1977] for which the  $B_z$  event was delayed by 15 hours. The delay of the southward IMF events from the leading edge of the interplanetary disturbances gives important clues as to the origin of the responsible interplanetary magnetic fields.

Several works have focused on the interplanetary phenomena associated with the large southward IMF events. Klein and Burlaga [1982] have identified "magnetic clouds," which,

when oriented in the vertical direction, have large southward (then northward) field components (or vice versa). The criteria of a "cloud" are a radial dimension of  $\sim 0.25$  AU at 1 AU, high,  $> 10$  nT, field magnitudes, and magnetic field directional changes by a rotation in a plane. Klein and Burlaga note that this field geometry is consistent with a magnetic loop or bubble [see Burlaga and Behannon, 1982] but cannot be uniquely determined because of the limitation of single-spacecraft measurements. In a sense the above classification is unfortunately too broad for the purpose of this present study. As examples, kinky heliospheric current sheets [Smith, 1981; Akasofu, 1981; Tsurutani et al., 1984, 1985] that are present in the compressed and heated plasma behind interplanetary shocks (which we hereafter call the "sheath" region) and draped interplanetary magnetic fields [Gosling and McComas, 1987] might also fit the general classification of a magnetic cloud. The fields may be sufficiently intense and the duration sufficiently long to meet Klein and Burlaga's criteria. The latter category, draped interplanetary fields, would have the configuration of a magnetic tongue, but would be caused by an entirely different process (see Gosling and McComas [1987] for discussion). Thus although we do not use the magnetic cloud categorization in this paper, for the above reasons, some of the southward field events presented are indeed "clouds." We will point this out to the reader where appropriate.

It is the purpose of this paper to use simultaneous ISEE 3 field and plasma information to determine the interplanetary phenomena associated with the 10 well-documented storm events identified in the work of Gonzalez and Tsurutani [1987]. These were all of the storm events with  $D_{st}$  magnitude of  $< -100$  nT during a continuous 500-day interval of 1978-1979. In this study we will attempt to determine whether the IMF southward field is caused by postshock turbulence, field draping, shocked kinky current sheets, driver gas magnetic fields (bubbles or tongues [Gold, 1962]) or other factors not previously hypothesized. The purpose of this effort is twofold:

<sup>1</sup>Jet Propulsion Laboratory, California Institute of Technology, Pasadena.

<sup>2</sup>Instituto de Pesquisas Espaciais, São Jose Dos Campos, Brazil.

<sup>3</sup>California Institute of Technology, Pasadena.

<sup>4</sup>Geophysical Institute, University of Alaska, Fairbanks.

Copyright 1988 by the American Geophysical Union.

Paper number 7A9404.  
0148-0227/88/007A-9404\$05.00

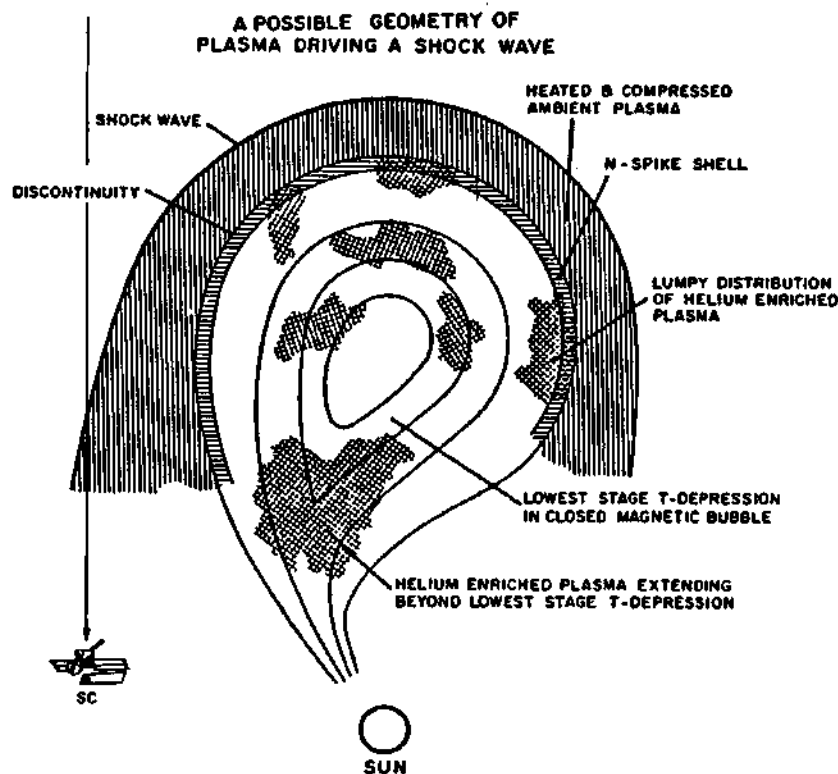


Fig. 1. Schematic model illustrating a possible geometry for plasma driving an interplanetary shock [from Bame *et al.*, 1979]. The "N spike" is a density enhancement that is sometimes observed at the boundary of the driver gas. There often are electron and ion temperature depressions ( $T$  depression) within the driver gas.

(1) to get a somewhat limited but statistical sample of the origins of the southward fields causing large magnetic storms and (2) in a future paper (F. Tang *et al.*, Solar sources of interplanetary southward  $B_z$  events responsible for major magnetic storms (1978–1979), submitted to *Journal of Geophysical Research*, 1988; henceforth referred to as Tang *et al.* (submitted manuscript, 1988)) to study the solar origins of the interplanetary events. We will also address the controversial topic of the possibility of predicting the orientation of interplanetary magnetic fields by using solar observations and simple radial convection of solar magnetic fields [Pudovkin and Chertkov, 1976; Pudovkin *et al.*, 1979; Pudovkin and Zaitseva, 1986; Tang *et al.*, 1985, 1986]. Clearly, only driver gas magnetic field events could possibly be predicted using ground-based solar observations. Events associated with the interplanetary "sheath" fields would be associated with the slow solar wind (whose origin is not well understood) or dynamical compression of such plasma and fields. Thus if a significant fraction of the storm events is caused by phenomena within the shocked interplanetary gases due to the interactions of high-speed streams and upstream slow streams, the statistical results of Pudovkin and Chertkov [1976] and Pudovkin *et al.* [1979] will need to be reevaluated due to their a priori assumption of knowledge of the solar origin of the interplanetary magnetic fields.

#### METHOD OF ANALYSIS

A 500-day interval (August 16, 1978, to December 28, 1979) was chosen such that there was a complete high time resolution data set available: magnetic field, solar wind electron,

proton and helium densities, temperatures, and anisotropies [Frandsen *et al.*, 1978; Bame *et al.*, 1978]. A complete plasma and field data set was necessary to identify shocks and driver gases. The interval starts at the spacecraft launch and ends near the failure of the ISEE 3 ion detector. In essence, essentially all of the complete data set available is used.

The driver gas, if present, will be identified by plasma and field characteristics cited by Zwickl *et al.* [1983]. As noted by Zwickl *et al.*, there is not a single set of parameters that will always be present in a driver gas. Depending on the spacecraft trajectory through the interplanetary shock and plasma driver, patches of enhanced helium may or may not be detected (the Bame raisin pudding model—see Figure 1). One can also note that it is easy to miss the driver gas if the spacecraft passes through the flank of the shock.

The 10 magnetic storm events that occurred during the interval of study are given in Figure 2. The figure contains information concerning the magnetic storm peak strength ( $D_m$ ), the interplanetary event which preceded the southward IMF (shock or no shock), and peak  $B_z$  values following the interplanetary events. The figure is taken from Gonzalez and Tsurutani [1987, Figure 2]. It can be noted that most, but not all (9 of 10 events), are preceded by interplanetary shocks. The one event that was not associated with a shock had a precursor density compression, possibly a noncompressional density enhancement (NCDE), as discussed by Gosling *et al.* [1977].

As previously mentioned, all magnetic storms were caused by large southward IMF ( $B_z < -10$  nT) events with long durations ( $\tau > 3$  hours). All of the peak southward  $B_z$  events occurred within 36 hours after the shock or NCDE passage.

# LARGE $D_{st}$ EVENTS ( $< -100$ nT) (AUG. 16, 1978 — DEC. 28, 1979)

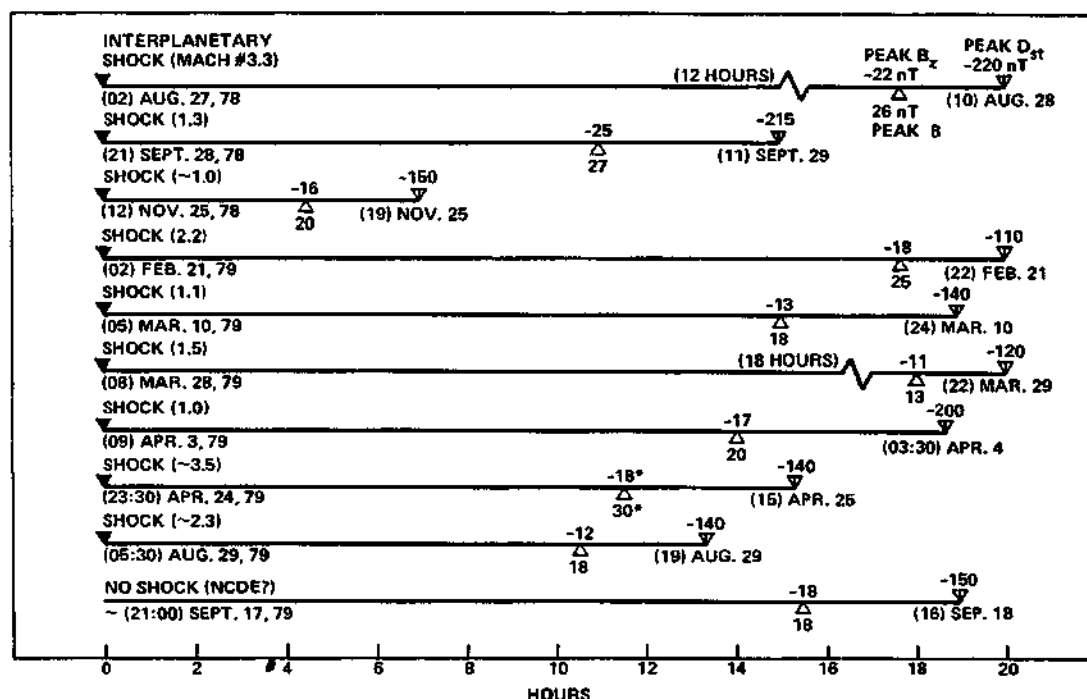


Fig. 2. Overview of the 10 large ( $D_{st} < -100$  nT) magnetic storms and associated interplanetary phenomena. This is taken from Gonzalez and Tsurutani [1987]. (Left to right) interplanetary phenomena detected prior to the large southward IMF events causing the magnetic storms (shock Mach numbers), peak southward  $B_z$  values, and IMF magnitudes and peak  $D_{st}$  values. All southward IMF events occur within 36 hours of a leading interplanetary shock (9 out of 10 events) or a noncompressed density enhancement event (one case).

The majority (7 of 10 events) occurred within 10–20 hours after the onset of the interplanetary disturbance. Of the other three events, one occurred 4 hours after a shock, and the others 30 and 36 hours after their precursor shocks.

Storm  $D_{st}$  developments do not always intensify in a monotonic fashion. This will be shown to be related to the presence of several interplanetary southward  $B_z$  events within the high-speed stream or NCDE event. Each southward turning causes a subsequent  $D_{st}$  decrease. To keep the accounting of the cause of the storm simple and straightforward, we will list the  $B_z$  event that causes  $D_{st}$  to reach  $-100$  nT first as the one responsible for the storm. Prior  $B_z$  events which do not quite lead to  $D_{st} = -100$  nT or subsequent  $B_z$  events which cause the storm to intensify will not be "counted." These events will, however, be cited both in the text and in the discussion for completeness.

## EVENT CASE STUDY

Since it is not possible to discuss and illustrate the features of all 10 events for this paper, we will show examples of five different types of southward  $B_z$  events and, at the end, give a summary of all 10 events.

### September 29, 1978 (Day 272)

Figure 3 illustrates the plasma, field, and geomagnetic activity associated with this event. From top to bottom are the helium density, proton temperature, velocity and density, the magnetic field GSE  $y$ ,  $z$ , and magnitude components, an 11-

station AE index, and  $D_{st}$  (see Baker et al. [1983] for discussion of the geomagnetic stations used for the construction of the geomagnetic indices). This same format will be used for all of the events shown.

The collisionless shock preceding the high-speed stream occurs at 2040 UT, day 271. This can be identified in the figure by the increase in proton density, velocity, temperature, and magnetic field intensity. The jumps are relatively small, consistent with a  $\sim M_s = 1.3$  shock strength determination (indicated in Figure 2). The shock normal was first calculated using the Abraham-Schrauner [1972] mixed mode method (which assumes the Rankine-Hugoniot relationships) using high time resolution magnetic field and plasma data. The shock velocity is determined by assuming conservation of mass flux [Tsurutani and Lin, 1985]. The shock Mach number is derived by calculating the upstream fast mode speed at the determined propagation angle. In this and other calculations the electron temperature is assumed to be  $1.5 \times 10^5$  K, and helium ions were neglected. Galvin et al. [1987] have reported that there was a second shock at  $\sim 0230$  UT occurring in the 3-hour telemetry gap. This shock was detected by Earth-orbiting spacecraft. An analysis of the properties of this shock at ISEE 3 is not possible.

The southward IMF responsible for the storm starts abruptly as a discontinuity at 0620 UT, day 272. The field turns northward at  $\sim 0800$  and southward a second time at 0813 UT. This second southward turning is the most intense and leads to the intensification of the storm (defined in this paper

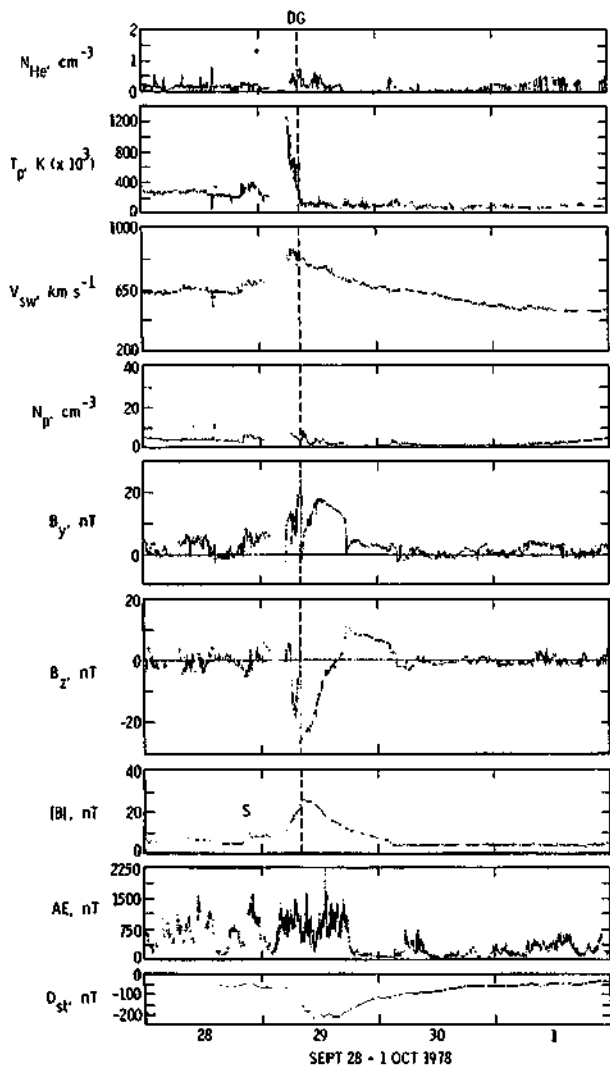


Fig. 3. The interplanetary field and plasma for the September 29–30, 1978, geomagnetic storm. The southward (and then northward) fields are located within the driver gas plasma. This field could be a magnetic bubble or tongue.

as  $D_{st} \leq -100$  nT). This occurs 11 hours, 33 min following the first shock. Figure 4 shows this in higher time resolution. The magnetic field  $z$  component decreases from +10 nT to -25 nT across the discontinuity. The magnetic field magnitude is  $\sim 25$  nT in the postdiscontinuity region, so the field is almost totally southward in direction. Afterward the field slowly rotates until it reaches a more northward orientation. At 1800 UT, day 272 (see Figure 3), it reaches a value of +12 nT. The slow decrease in the IMF southward component (starting at 0800 UT September 29) starts the recovery phase of the magnetic storm (see W. D. Gonzalez et al. (Solar wind-magnetosphere coupling during major magnetic storms of 1978–1979, submitted to *Journal of Geophysical Research*, 1988) for detailed discussion).

The plasma and fields at and after the discontinuity are consistent with their being part of the driver gas plasma. The discontinuity has been analyzed using a principal axis analysis program [Smith and Tsurutani, 1976] applied to high time

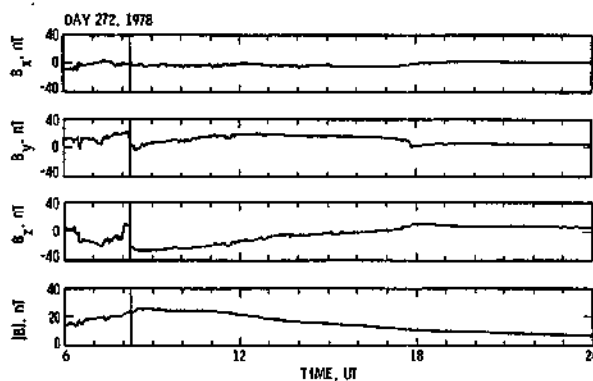


Fig. 4. The high-resolution magnetic field at and after the discontinuity bounding the shocked sheath plasma from the driver gas plasma. High-intensity fields with low variances (after 0813 UT) identify this as part of the driver gas. The magnetic field after the discontinuity is strongly southward. This is the cause of the development of the geomagnetic storm.

resolution (6 vectors/s) data. The field across the discontinuity has been transformed to the principal coordinate system and is shown in Figure 5. The angle between the normal to the discontinuity and the magnetic field is  $73^\circ$  ( $B_n/B = 0.29$ ). The field in the minimum variance direction ( $B_3$ ) is constant, indicating an accurate determination. It has a small but definitely nonzero value, implying a rotational discontinuity. The field in the maximum variance direction ( $B_1$ ) changes in two steps, similar to the event previously shown and discussed in detail by Unti et al. (1972). The above authors interpreted this as magnetic reconnection occurring across the discontinuity.

The magnetic field is very smooth (low variances) after the discontinuity (shown in Figure 4). The field magnitude de-

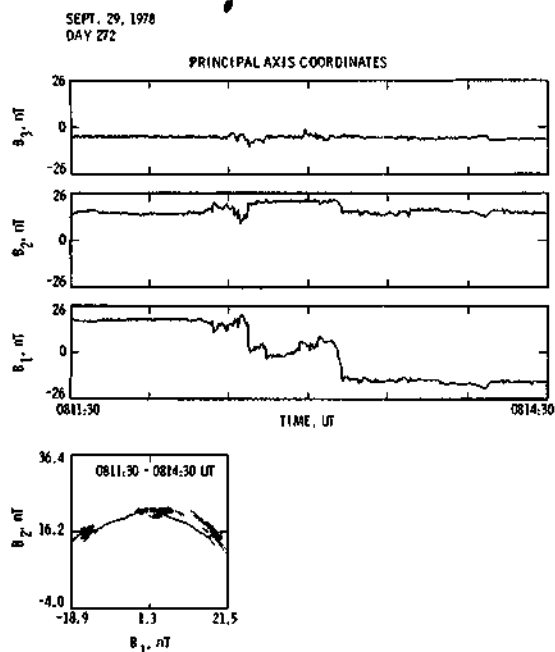


Fig. 5. The 0813 UT discontinuity in principal axis coordinates and a hodogram of the vector rotation in the  $B_1 - B_2$  plane. There is a small but constant field component in the discontinuity normal direction ( $B_3 = B_n = 0.29|B|$ ). This is a rotational discontinuity.

creases monotonically until 0250 UT, day 273 (not shown), when the field becomes more turbulent, thus ending the clearly identifiable driver gas [Zwickl *et al.*, 1983; Smith *et al.*, 1986]. Most of the plasma parameters also fit the identification of a driver gas as given by Zwickl *et al.* [1983]: there are (small) proton density and temperature decreases across the discontinuity. The helium density becomes higher near the discontinuity but possibly somewhat ahead of the discontinuity (see an excellent detailed discussion of the ion charge states in this region by Galvin *et al.* [1987]).

From the above, we have identified the southward IMF responsible for the magnetic storm as the magnetic field within the high-speed stream driver gas. The sudden turning of the field toward the southward direction occurs at the discontinuity separating the shocked solar wind plasma from the driver gas plasma [see Galvin *et al.*, 1987]. The southward-then-northward characteristic indicates that this event may possibly be a Klein and Burlaga "magnetic cloud"—a closed bubble or magnetic tongue [Gold, 1962] extending from the Sun. Gosling *et al.* [1987] have indicated the presence of a bidirectional solar-wind electron heat flux during this event, arguing for magnetic closure.

November 25, 1978 (Day 329)

This southward IMF event begins exactly at the shock located at 1140 UT, day 329. This is shown in Figure 6. The shock is clearly identifiable by jumps in  $T_p$ ,  $N_p$ ,  $V_{sw}$ , and  $|B|$ . The jumps in the plasma parameters are small, and the calculated shock magnetosonic Mach number is approximately 1.0, indicating a very weak event. The upstream IMF had a  $-7$ -nT  $B_z$  component (out of an 8-nT field), and the shock compression causes a downstream  $B_z$  value of  $-10$  nT (further increasing to  $-15$  nT in time), in agreement with a weak shock. Thus the field responsible for the magnetic storm is simply shocked interplanetary magnetic fields. The southward IMF ends sharply with a discontinuity at 1714 UT, day 329. There is a constant normal component of the field across the discontinuity ( $0.27|B|$ ), and the magnetic field magnitude remains relatively constant. The hodogram in Figure 7 shows a clear rotation indicating it is a rotational discontinuity. The antisunward (upstream) side of the discontinuity is characterized by high proton and helium densities (Figure 6, first and fourth panels), which abruptly decrease across the discontinuity. A substantial proton temperature increase is found at the discontinuity. The discontinuity is located approximately midway between the forward shock (1140 UT) and a reverse shock at 0140 UT, day 330. The reverse shock is identified by a velocity increase, temperature and density decrease, and magnetic field decrease. For more details concerning the jump conditions across collisionless shocks, see Tidman and Krall [1971] and Stone and Tsurutani [1985].

The interplanetary event appears to possibly be a corotating structure. Previous appearances of shocks are observed on September 5, October 3, October 29, and an event following the November 25 event, December 21. Thus the discontinuity ending the southward field event discussed above could be the stream-stream interface of the corotating interaction region [Smith and Wolfe, 1976; Gosling *et al.*, 1976]. The event has the classic corotating interaction region (CIR) "boxcar" shape: a forward shock and reverse shock bounding the intense fields with a discontinuity in the middle separating the fast plasma from the shocked slow plasma [Smith and Wolfe, 1976]. There is also no evidence of the presence of a driver gas. On the other hand, this event could be produced by a coronal mass

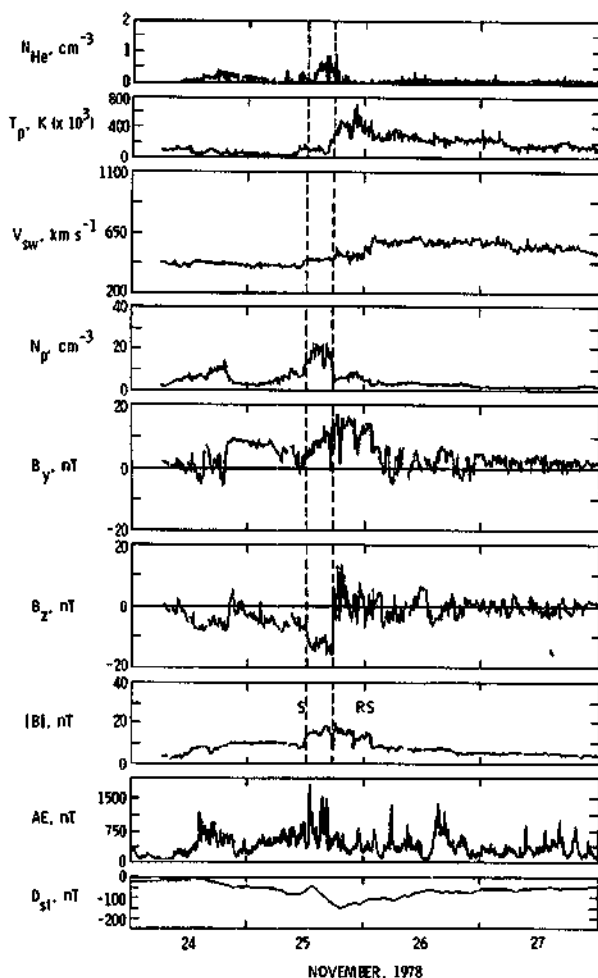


Fig. 6. The interplanetary magnetic field and plasma for the November 24–26, 1978, geomagnetic storm. As indicated by the  $D_{st}$  value, the magnetic storm was ongoing at a relatively intense level prior to the interplanetary shock and high-speed solar wind stream that was detected at 1140 UT November 25. The ongoing activity was caused by the southward interplanetary magnetic field that was present in the quiet solar wind prior to the shock arrival. The interplanetary shock compressed and intensified the preexisting southward fields, leading to storm intensification to  $D_{st}$  values of  $< -100$  nT. Note the presence of fluctuations in the  $B_y$  and  $B_z$  components (Alfvén waves) and resultant high-latitude AE activity during the recovery phase of the storm (November 26 and 27). Such Alfvén waves and AE activity were not present in the recovery phase of the September 29, 1978, storm (Figure 3).

ejection event which is centered away from the Sun-Earth line (see discussion by Cane [1988]), such that the driver gas is missed. An additional argument for this hypothesis is that forward and reverse shocks associated with corotating streams do not generally form until  $\sim 1.5$  and  $2.5$  AU, respectively [Smith and Wolfe, 1976], considerably more distant from the Sun than the present event.

One final comment about this event concerns the effect of the southward  $B_z$  prior to the interplanetary shock. Note that this "quiet" interplanetary field led to  $D_{st}$  reaching values of  $-80$  nT. Thus if one uses less stringent requirements for magnetic storms (say,  $D_{st} < -50$  nT), presumably there will be many events of this type.

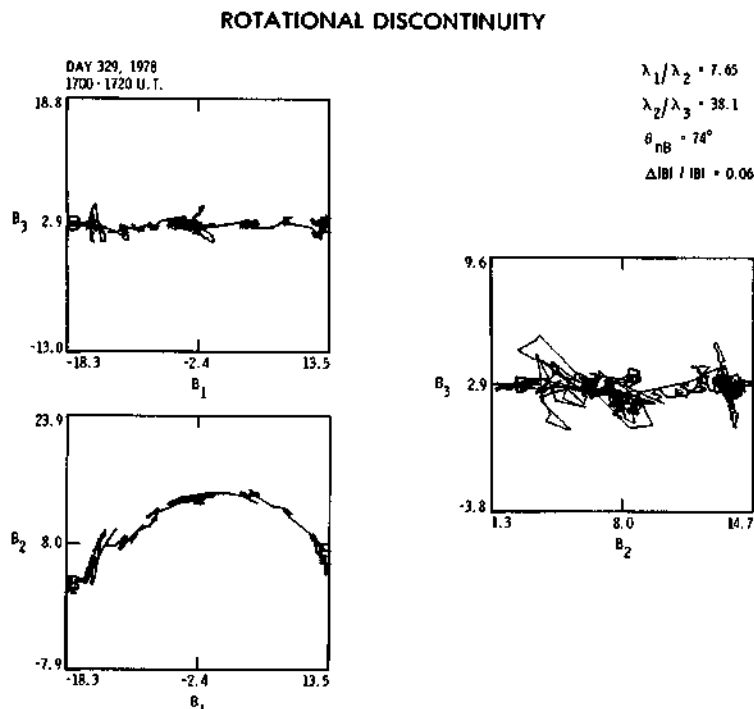


Fig. 7. High-resolution magnetic fields illustrating the discontinuity associated with the termination of the November 25, 1978, magnetic storm. The large constant normal component ( $B_3$ ) and constant magnitude across the discontinuity indicate it is a rotational discontinuity. This discontinuity is believed to be the interface between the high and slow stream plasmas.

April 4, 1979 (Day 94)

The shock which precedes the southward  $B_z$  event occurs at 0925 UT, day 93. This is illustrated in Figure 8 and is taken from Gonzalez and Tsurutani [1987]. The upstream northward directed IMF is intensified at the shock from +2 nT to +7 nT. The Mach number is determined to be  $\sim 1.0$ . Note that a far more intense shock (and high-speed stream) follows on day 95 which does not cause intense geomagnetic activity. The reason for this is that the magnetic field which follows is primarily northward (see Gonzalez and Tsurutani [1987] for more details).

There are three important broad directional "discontinuities" following the shock which bracket important  $B_z$  changes and will be discussed below. They are the first southward turning at 1430–1450 UT, day 93, a second, deeper southward (complex) event at  $\sim 1930$ –2020 UT, day 93, and a third broad "discontinuity" at 1818–2026 UT, day 94. The first of the three discontinuities is responsible for the start of the magnetic storm but causes it to reach a magnitude of only  $D_{st} \sim -90$  nT. Because of our method of accounting for the cause of the magnetic storm discussed previously, this southward IMF event will not be listed as the responsible source. The following deeper southward  $B_z$  event at  $\sim 1930$ –2020 UT which causes  $D_{st}$  to reach  $< -100$  nT will be listed as the event responsible for the magnetic storm.

The first "discontinuity" is quite broad, lasting from 1430 to 1450 UT. As can be noted in Figure 8, it is accompanied by a density decrease and temperature increase without any change in  $B$  magnitude. Principal axis analyses indicate that this is a tangential discontinuity with  $\theta_{nB} = 77^\circ$ . There are no en-

hanced helium values throughout the event ( $N_{He}/N_p < 0.05$ ). This does not appear to be a discontinuity at the edge of a driver gas. One interpretation is that this is a discontinuity that has been swept up and compressed in the solar wind interaction region. This conjecture will be strengthened by the discussion below.

The second "discontinuity" is also thick, lasting from 1930 UT to 2020 UT. It is accompanied by a sharp, intense spike in  $N_p$  and a  $|B|$  enhancement. The proton temperature is low following the discontinuity, and the magnetic field relatively quiet. The discontinuity has a normal component of  $0.31|B|$ , and the field magnitude change across the discontinuity is substantial,  $\sim 3$  nT out of a 15-nT total field. There is a substantial field decrease in the center of the discontinuity (to 12 nT), indicative of an intense current sheet. All of the above criteria identify this as the discontinuity bounding the driver gas of the high-speed stream.

The third "discontinuity" at 1818–2026 UT causes reduction of the large northward  $B_z$  component to a value near zero. There is a small normal component across the discontinuity ( $B_z = 0.30|B|$ ), with little or no change in field magnitude. It should be noted that this "discontinuity" is actually composed of two very sharp discontinuous changes. They occur at 1818:00 and 2023:36 UT and are quantitatively similar to the Unti et al. [1972] event.

If one considers the interval between the second and third "discontinuities," there is an initial, abrupt southward field at the second discontinuity, a gradual rotation in direction toward the north, then a cutoff at the third discontinuity. This overall field rotation and structure is consistent with a magnetic cloud contained within the driver gas.

The southward field of the driver gas (second discontinuity) is responsible for the magnetic storm. The sheath southward fields led to a  $D_{st}$  of only  $-90$  nT.

August 29, 1979 (Day 241)

The shock occurs in a data gap around 0500 UT, day 241, as indicated by the jump in the proton temperature, density, velocity, and magnetic field following the gap (Figure 9). From an analysis of the high-resolution upstream and downstream plasma and field data the magnetosonic Mach number is determined to be 2.3. The shock intensifies a presumably preexisting northward field (within the data gap just preceding the shock). A southward turning occurs from 0700 to 0725 UT, day 241, just behind the shock. The field stays primarily

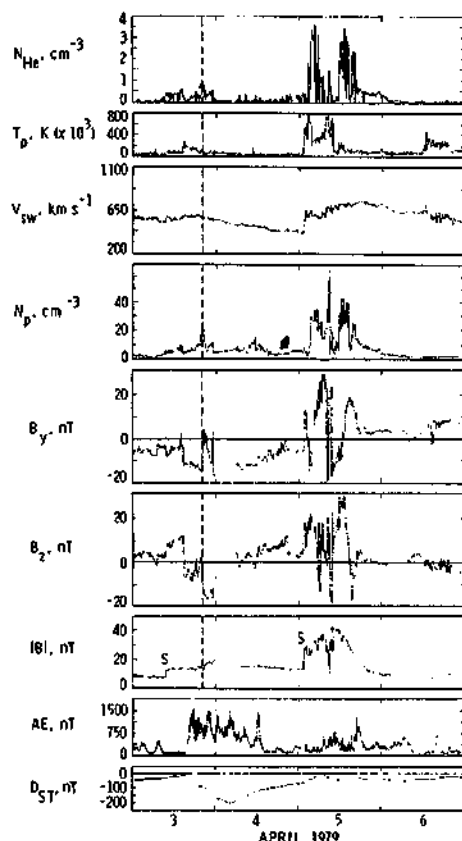


Fig. 8. The interplanetary magnetic field and plasma for the April 3-4, 1979, magnetic storm. A broad discontinuity at 1430-1450 and trailing southward fields are responsible for the onset of the magnetic storm and cause it to reach a  $D_{st}$  magnitude of  $< -90$  nT. The discontinuity appears to be a tangential discontinuity with  $\theta_{Bn} = 77^\circ$ . One interpretation is that this is a discontinuity that has been swept up and compressed (and distorted) in the solar wind interaction region. Another thick discontinuity occurs about 5 hours later, 1930-2020 UT. The proton temperature is low, and the magnetic field intensity is high(er) and quiet following the discontinuity. This discontinuity is thus believed to bound the driver gas plasma. The IMF following the discontinuity has a south-then-north rotation, consistent with a magnetic tongue or bubble. The driver gas fields are responsible for the storm reaching  $D_{st}$  intensities of  $\leq -200$  nT. Note the much more intense interplanetary shock event on April 5, following the April 3-4 magnetic storm recovery. Because there are not long-duration southward fields associated with the second high-speed stream (the fields are primarily northward), the geomagnetic activity is a minimum (see discussion by Gonzalez and Tsurutani [1987]).

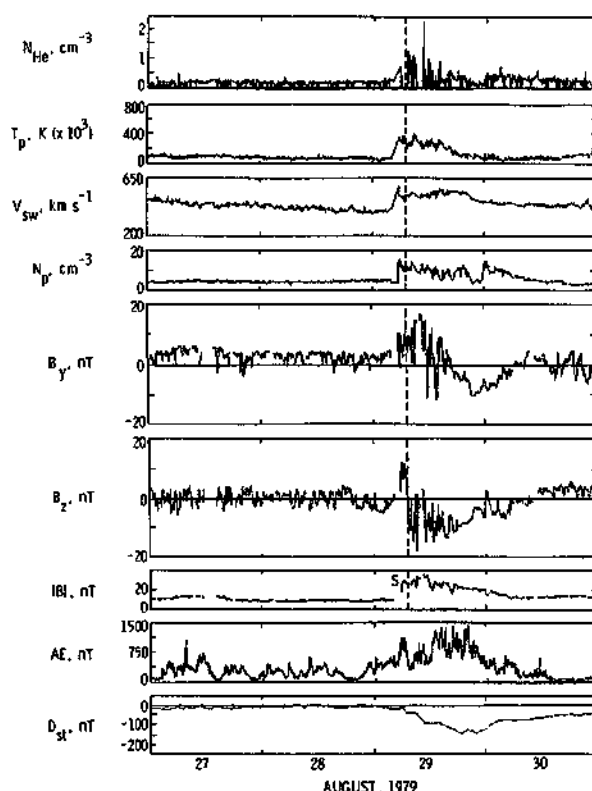


Fig. 9. The interplanetary magnetic field and plasma for the August 29-30, 1979, geomagnetic storm. The southward magnetic fields which cause the magnetic storm start at 0700-0725 UT, just 2 hours after the shock ( $\sim 0500$  UT). From the location (relative to the shock) and the character of the field and plasma the southward fields are part of the magnetosheath plasma. Arguments are presented indicating that the abrupt change in the field direction is either a crossing of the heliospheric current sheet or a distorted and compressed interplanetary discontinuity.

southward after this time but is highly variable in nature. This can be seen in the large-amplitude fluctuations in the  $B_y$  and  $B_z$  components shown in the figure. This fluctuating southward is correlated with and presumably responsible for the magnetic storm.

Gosling and McComas [1987] have discussed this interplanetary event and indicated that there is a possibility of the presence of driver gas starting at  $\sim 1800$  UT, day 242. This occurs at the time of the peak  $D_{st}$  value and is associated with the recovery phase of the magnetic storm. The storm initiation and intensification are due to the shocked fields discussed previously. The fields and plasmas after 1800 UT are somewhat different, and the evidence for a driver gas is present, but not particularly compelling. Within the region where the fields are southward (0725-2000 UT) the proton temperature is high, the density is high, and the He/H ratio is typical of the solar wind,  $< 5\%$ . Gosling and McComas indicate that the proton temperature drops just after the discontinuity. However, it is initially at values above the upstream slow solar wind stream and is not unusually low. The magnetic field is relatively quiet (but not as quiet as shown in Figure 4) from 1800 to 2400 UT. After this interval the field is typical of the regular solar wind.

The magnetic field orientation for this  $B_z$  event is shown in higher time resolution (1-min averages) in Figure 10. The plots

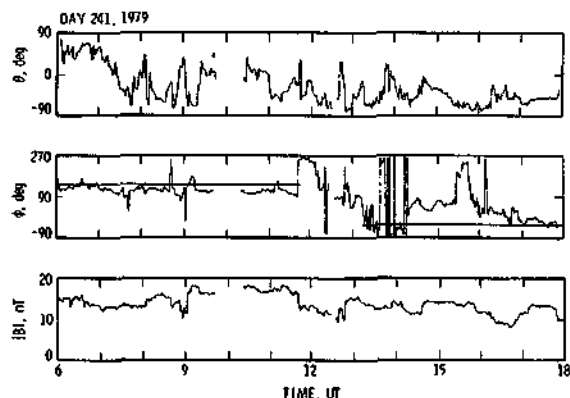


Fig. 10. The "sheath" fields in GSE polar coordinates. The multiple switching of the  $\phi$  angle from  $\sim 135^\circ$  to  $315^\circ$  indicates changing from a positive (outward) Parker spiral direction to a negative (inward) spiral direction. Multiple crossings of the heliospheric current sheet provide one possible explanation; swept up interplanetary discontinuities and waves are another.

are given in GSE polar coordinates. In this system,  $\phi$  has a value  $0^\circ$  toward the Sun and increases with the sense of the rotation of the planets about the Sun. Thus  $\phi = 135^\circ$  and  $-45^\circ$  correspond to positive and negative polarity interplanetary magnetic fields, respectively (denoted by solid lines). The north ecliptic pole is at  $\theta = 90^\circ$ . From 0600 to 1130 UT the magnetic field was in a Parker spiral configuration with strong out-of-the-ecliptic components. This includes the 0700–0725 UT interval where the southward turning of the field led to the onset of the geomagnetic storm. From 1200 to 1600 UT,  $\phi$  varied considerably but often had values near  $-45^\circ$ . The latter is consistent with negative sector fields. Thus one possible interpretation of this event is that the fields represent multiple crossings of a distorted heliospheric current sheet. On the other hand, the current sheet crossing at the sun occurred on August 20, some 9 days earlier, detracting from this interpretation. A more probable interpretation is that the southward turning is an interplanetary discontinuity that has been swept up, compressed (and distorted) by the interplanetary shock. Gosling and McComas [1987] have concluded that this event is a draped magnetic field event, consistent with the above interpretation. This event has also been listed as a magnetic cloud by Burlaga et al. [1987].

#### September 18, 1979 (Day 261)

This event is illustrated because it is unexpected, according to "conventional wisdom." There is no shock preceding the event. There is also not a high-speed solar wind stream with trailing driver gas or with an interaction region (with the upstream slower speed stream providing the highly compressed magnetic fields) necessary for the identified interplanetary criteria causing magnetic storms,  $B_z \leq -10$  nT for over 3 hours. The velocity, shown in the third panel of Figure 11 [from Gonzalez and Tsurutani, 1987, Figure 4], remains under 425 km/s throughout the entire magnetic storm. Although this is the only event of this type found in the interval of study, it is one of the 10 events analyzed (10%). It should be pointed out that for high-intensity, long-duration continuous AE (substorm) events (HILDCAAs) caused by interplanetary Alfvén wave trains [Tsurutani and Gonzalez, 1987], similar interplanetary events (led by large density enhancements) were again nonnegligible, representing three of eight occurrences (37%). Thus, NCDEs may be a very important, relatively unexplored

solar wind phenomenon that can have major impacts on geomagnetic activity. Further study of the causes and effects of NCDEs are needed.

The interplanetary density enhancement that precedes the southward field event starts gradually at  $\sim 900$  UT, day 260. The noticeable features are both the gradual density and magnetic field magnitude increases to unusually high values from the "quiet" solar wind ( $3\text{--}10\text{ cm}^{-3}$ ). The proton density is characterized by two very large density spikes reaching values up to  $35\text{ cm}^{-3}$ . These occur at  $\sim 2300$  UT, day 260, and  $\sim 0500$  UT, day 261. Between the two density peaks is a local minimum. The interval from the onset of the first density peak to the density minimum is associated with a large southward IMF event. However,  $D_{st}$  does not become less than  $-100$  nT due to this event. Because the southward IMF event does not

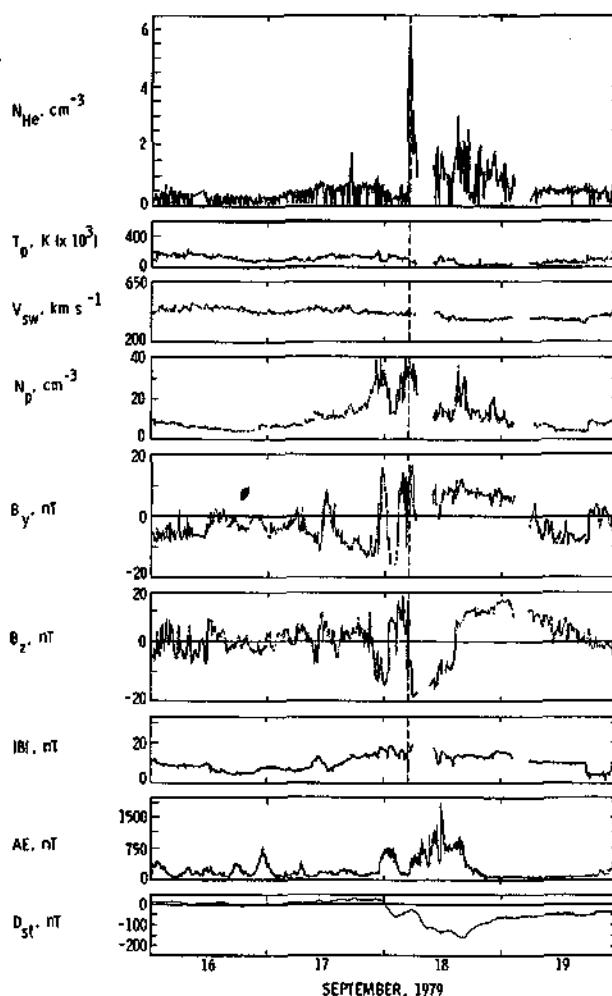


Fig. 11. The interplanetary magnetic field and plasma for the September 18, 1979, geomagnetic storm. This geomagnetic storm is not caused by magnetic fields associated with a high-speed solar wind stream (and shock). The high (southward) fields causing the magnetic storm start in the middle of the second of two unusually large density spikes ( $N_p \approx 35\text{ cm}^{-3}$ ). This is indicated by the dashed vertical line. One possible interpretation is that the southward fields are created by draping over the high-density plasma (see schematic of Gosling and McComas [1987]). Another possible scenario is that these fields are part of the driver gas of a coronal mass ejection that has the same velocity as the upstream solar wind.



cause the magnetic storm, we will not discuss it further. There is a broad discontinuity from 0400 to 0600, day 261, that is associated with the trailing edge of the second major interplanetary density enhancement. The magnetic storm is primarily caused by the very intense, long-duration southward  $B_z$  event that follows this southward turning (Figure 12). The southward field event ends abruptly at 1435 UT, day 261, with a directional discontinuity. The responsible IMF  $B_z$  onset is very broad, characterized by intense fluctuations. It is not a discontinuity in the classical definition. The IMF  $B_z$  termination is caused by a rotational discontinuity at 1435 UT. The discontinuity has a very large normal  $B_n = 0.67|B|$  and no change in field magnitude across its surface. The magnetic field throughout this interval is not particularly quiet.

One possible interpretation of the southward field event is that it is caused by magnetic fields draped over the high-density regions. At 1800 UT, day 260, prior to the first density enhancement,  $B_x > 0$ , and  $B_y < 0$ , consistent with a negative IMF polarity. From 1800 to 2400 UT,  $B_x$  decreases to a value of zero. The  $B_y$  component has a positive component from  $\sim 2300$  UT, day 260, to  $\sim 0025$  UT, day 261, correlated with the (first) proton density enhancement. The second proton density enhancement is again correlated with strong and positive  $B_y$  components. The onset occurs at 0230–0245 UT, and the termination is near 0600 UT. The latter time is coincident with the onset of the IMF  $B_z$  event which is responsible for the magnetic storm.

We mention other features of this event for completeness. The interval 0400–0500 UT, day 261, has characteristics that are very similar to the driver gases discussed previously. The He/H ratio is specifically quite high ( $> 10\%$ ), and the proton temperature is very low. From 0600 UT, day 261, to 0130 UT, day 262, the magnetic field is intense and relatively devoid of waves and discontinuities. The characteristic south-north rotation of the magnetic field identifies this as a magnetic cloud. However, it should be mentioned that the high helium densities occur in the middle of the second proton density enhancement and there is no discontinuity associated with the onset.

#### Other Events

The above is a description of 5 of the 10 events. Below we will describe the other five events briefly and, for brevity, without illustration.

**August 27, 1978 (day 239).** This magnetic storm event is initiated by a broad southward turning at  $\sim 2000$  UT, day 239. This is preceded by a sharp discontinuity at 1826 UT. The discontinuity has a normal component equal to  $0.06|B|$ . The field magnitude change across it is  $0.15|B|$ . The event is a tangential discontinuity. The fields behind are smooth, identifying it as possible driver gas plasma. However, the proton temperatures and densities are not particularly low, nor is the He/H ratio high.

Based on the magnetic fields alone, this IMF southward event will be labeled as being related to driver gas plasma. The magnetic fields, however, only have a southward component. There is no northward component for a "magnetic cloud," as described by Klein and Burlaga [1982]. The  $B_y$  component does have a negative-then-positive characteristic, so one possibility is that this could be a cloud that is highly tilted. In support of the closed magnetic field picture, Gosling et al. [1987] have indicated bidirectional electron heat flux from 1000 UT August 27 to 0200 UT August 28.

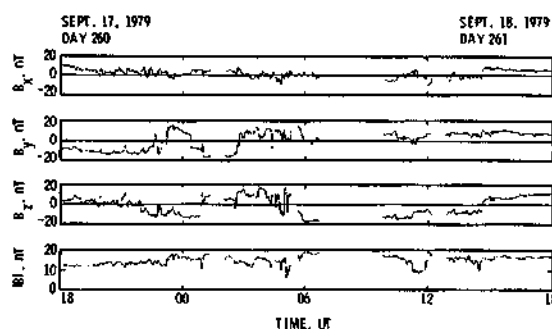


Fig. 12. The high-resolution interplanetary magnetic field for the September 18, 1979, event.

It should be noted that this event is associated with a "compound stream." There are two and maybe three high-speed streams involved. The proton densities reach values of  $> 40 \text{ cm}^{-3}$ . For further discussion of compound streams see Burlaga et al. [1987].

**February 21, 1979 (day 52).** This event has two major southward events, similar to many of the previous examples illustrated. The first event is initialized immediately behind the shock at  $\sim 0240$ – $0330$  UT (the shock is at 0220 UT) and lasts until  $\sim 0800$  UT. This causes a substantial decrease in  $D_{st}$  to a maximum of  $-90$  nT. The IMF  $B_z$ - $B_y$  components remain relatively consistent throughout this  $B_z$  event.  $B_x < 0$ , implying a positive Parker orientation. It is unlikely that the  $B_z$  event is a twisted heliospheric current sheet, but most probably it is a shock-intensified discontinuity or locally generated field distortion event.

The second major event starts at 1501 UT and ends at 2035 UT. This second major  $B_z$  event is responsible for the magnetic storm with  $D_{st} \leq -100$  nT. The onset of the southward IMF event is caused by a discontinuity with  $B_n/|B| = 0.37$ , and the field magnitude change is  $-6$  nT in a  $21.5$ -nT background. From the Smith [1973] criteria the discontinuity is presently identified as "indeterminate," having properties of both a rotational discontinuity and a tangential discontinuity [Landau and Lifshitz, 1960]. Further analyses of high-resolution field and plasma data will have to be performed to determine whether more can be learned about the nature of this particular discontinuity [see Neugebauer et al., 1984]. The He/H ratio, behind the discontinuity, is often  $> 10\%$ , and the temperatures are low, identifying it as driver gas. The magnetic field is quieter than usual but not as quiet as some of those previously illustrated.

**March 10, 1979 (day 69).** The storm is associated with a multiple high-speed stream structure with the IMF  $B_z$  event associated with the (compound) stream. The first stream is led by an interplanetary shock at 0723 UT, day 68. The second complex stream starts at  $Z \sim 2130$ – $2330$  UT, day 68. There is no shock associated with this event. The responsible IMF  $B_z$  event has an abrupt onset at 1800 UT, day 69, and gradually terminates at  $\sim 0500$ – $0600$  UT, day 70. The discontinuity has a very small normal component  $B_n = 0.0075|B|$ , and the field magnitude change across the discontinuity is unusually large,  $\sim 13$  nT in a  $14.8$ -nT ambient field. This is a tangential discontinuity.

From 0600–1000 UT, day 69,  $B_x > 0$  and  $B_y < 0$ , or the field has a negative sector polarity; from 1100–1300 UT,  $B_x < 0$  and  $B_y > 0$ , or the field has a positive sector polarity. From  $\sim 1500$  to 1800,  $B_x \sim 0$  nT, and the entire field lies along the  $y$

direction. At the discontinuity at 1800 UT,  $B_x$  becomes slightly negative,  $B_y \sim 0$  nT, and  $B_z \approx -12$  nT. At 2235–2249 UT there is a broad discontinuity, and  $B_y$  again changes from  $-10$  to  $-15$  nT to  $+15$  nT.  $B_z$  remains intensely negative throughout the interval. The field has orientations reasonably close to the Parker spiral prior to the IMF  $B_z$  event. Switching of  $B_x$  and  $B_y$  values indicates possible crossings of the heliospheric current sheet. However, during the  $-B_z$  event the fields have highly unusual orientations. The distortions presumably are due to the stream-stream interaction.

There is little evidence that this storm event is associated with driver gas fields. At the onset of the  $B_z$  discontinuity the helium density decreases, and the proton temperature increases slightly. The magnetic fields are not particularly quiet. The solar wind velocity increase may imply that this is the interface of another stream within the second (complex) event.

**March 29, 1979 (day 88).** This is a complex interplanetary event possibly composed of two high-speed streams. The first starts with a shock at 0754 UT, day 87. The second, smaller stream has a gradual onset at  $\sim 0400$  UT, day 88. The southward IMF event responsible for the storm is a dual event which occurs during the second solar wind stream. The first event starts abruptly at 0448–0500 UT, day 88, and lasts until 0800 UT. The second event starts gradually at  $\sim 0900$  UT and lasts until an abrupt northward turning at 2023 UT. The first southward event drives  $D_{st}$  to  $-100$  nT, and the second to  $-125$  nT. One may again call this two separate storms, but for simplicity we will only consider it as one and will concentrate on the first event which leads to  $D_{st}$  values of  $< -100$  nT, the criteria in the Gonzalez and Tsurutani [1987] study. In actuality the field data show that the interval 0800–0900 is only a gradual deflection of the field in the northward direction and then southward again, possibly a kink in the heliospheric current sheet.

The onset and termination of the southward events have been examined using principal axis analyses. Both are found to be rotational discontinuities. The first event has a normal component equal to 0.99 times the ambient field strength. The "wave" is propagating at an angle of  $5^\circ$  relative to  $B$ . There is little field magnitude change across the discontinuity.

The second southward event initiated at 0900–1000 UT is accompanied by smooth magnetic fields and a broad density spike followed by low temperatures. The event is terminated by a tangential discontinuity at 2023 UT, day 88. The magnitude is constant across the discontinuity, and  $\theta_{bn} \approx 37^\circ$ . The field behind the discontinuity is quiet. However, other than this feature there is no further evidence for a driver gas. The temperature and densities are normal, and there is no helium enhancement.

Our conclusion is that the initial southward  $B_z$  occurs on the rising portion of the stream, ahead of any possible driver gas. It appears as if it is caused by distorted, shocked interplanetary plasma, possibly the heliospheric current sheet.

**April 25, 1979 (day 115).** This is apparently a two-step southward  $B_z$  event (due to tracking limitations, there are large data gaps within these events). The  $D_{st}$  also has two corresponding decreases,  $-125$  nT and  $-145$  nT, respectively. Since the first  $D_{st}$  decrease is above  $-100$  nT, as before, we will focus on this event as the cause of the magnetic storm.

A forward shock occurs at 2325 UT, day 114, 1979. Substantial increases in field magnitude (up to 26 nT), density ( $20 \text{ cm}^{-3}$ ), velocity (750 km/s), and temperature ( $T_p \approx 8 \times 10^5 \text{ K}$ ) identify the Mach 3.5 shock. The  $B_z$  component becomes large and positive at the shock ( $+18$  nT) and becomes negative just

behind the shock ( $-15$  nT at 0100 UT, day 115). The data gap between 0130 and 0600 UT prevents further knowledge of the IMF variations. Presumably, because of the closeness of the southward field event to the shock the southward fields are shocked plasma that has been swept up by the fast stream.

Sudden spikes in H and He densities occur at  $\sim 0700$  UT, day 115. Values of  $>75 \text{ cm}^{-3}$  and  $>2 \text{ cm}^{-3}$ , respectively, were detected. A solar wind velocity increase of  $\sim 75$  km/s occurs coincident with the density spikes, but the magnetic field is variable and shows no clear trend. Large,  $\pm 20$ -nT  $B_z$  transients are associated with the interval near the density increases, possibly ending the first  $B_z$  event. The second southward turning starts somewhere in the middle of the (second) data gap and terminates from a slow northward turning at 1100–1130 UT. This is accompanied by decreases in the H and He densities.

An abrupt discontinuity occurs at 1250 UT, day 115, after the second  $B_z$  event has terminated. This discontinuity is either a weak reverse shock or a tangential discontinuity at the leading edge of the driver gas. A substantial field decrease occurs at the discontinuity (from 27 nT to 15 nT within 1 s). There is a very slight ( $<50$  km/s) rise in  $V_{sw}$  and decreases in helium and proton densities across the discontinuity. However, the sharpness of these changes cannot be determined because of the data gap following the discontinuity. The magnetic field magnitude change across the discontinuity is extremely sharp ( $<1$  s), supporting the possibility of a shock. There are high-frequency waves emanating from the discontinuity. The field normal to the discontinuity is  $B_n = 0.51|B|$ , again consistent with a shock. On the other hand, the fields from 1245 to 1900 UT are very smooth, and the proton density and temperatures are quite low, consistent with a driver gas. Further study will be needed to determine the cause of this event. This event was listed as a magnetic cloud by Burlaga et al. [1987].

#### EVENT SUMMARY

A summary of all of the 10  $B_z$  events is given in Table 1 and pictorially illustrated in Figure 13. The causes of the negative  $B_z$  events responsible for the storms are quite diverse and complex. Four of the storm intensifications (to  $D_{st} < -100$  nT) were related to driver gas magnetic fields: August 27, 1978; September 29, 1978; February 21, 1979; and April 4, 1979. Of the other six events, one is a shock field intensification event (November 25, 1978), possibly one or two (March 10, 1979, and August 29, 1979) are caused by kinky heliospheric current sheets, three or four are due to turbulent (sheath) magnetic fields behind the interplanetary shock (March 10, 1979; March 29, 1979; April 25, 1979; and August 29, 1979), and one event is due to draped fields or driver gas fields associated with a NCDE (September 18, 1979). The above breakdown is, of course, quite simplistic. It only focuses on the causes of the storms reaching  $D_{st} < -100$  nT. Many storm events were two-step processes (or more). One event had an initial major southward  $B_z$  event that initiated the storm and led to  $D_{st}$  intensities of  $-80$  nT (November 25, 1978). Two other sheath events prior to driver gas fields led to  $D_{st} \approx -90$  nT (February 21, 1979, and April 4, 1979). Driver gas events following two sheath events (which caused storm developments) were associated with storm intensifications to  $D_{st}$  levels of  $-125$  nT and  $-145$  nT (March 29, 1979, and April 25, 1979). The sheath events were credited with the cause of the storm intensifications for these events. Thus it is obvious that if one changes the threshold in the definition of a magnetic storm, considerably different statistics may result.

TABLE 1. Summary of the Interplanetary Phenomena Causing the 10 Large ( $Dst < -100$  nT) Magnetic Storm Events Occurring Near Solar Maximum

Date	Day	Time of IMF $B_z$ Onset (at ISEE 3)	Phenomenon
Aug. 27, 1978	239	1826 UT	driver gas
Sept. 29, 1978	272	0813 UT	driver gas
Nov. 25, 1978	329	1140 UT ( $-B_z$ prior to shock leads to $D_{st} = -80$ nT)	shocked $-B_z$
Feb. 21, 1979	52	1501 UT (kinky current sheet in magnetosheath leads to $D_{st} = -90$ nT; onset 0240–0330 UT)	driver gas
March 10, 1979	69	1800 UT	distorted sheath fields (current sheet?)
March 29, 1979	88	0448–0500 UT (possible driver gas leads to $D_{st}$ intensification to $-125$ nT; onset 0900 UT)	distorted sheath fields
April 4, 1979	94	1930–2020 UT (compressed interplanetary discontinuity in magnetosheath leads to $D_{st} = -90$ nT; onset 1430–1440 UT)	driver gas
April 25, 1979	115	0100 UT (driver gas? causes intensification to $D_{st} = -145$ nT; onset 1245 UT)	distorted sheath fields
Aug. 29, 1979	241	0700–0724 UT	distorted sheath fields (current sheet?)
Sept. 18, 1979	261	0400–0600 UT	draped fields/driver gas

## CONCLUSIONS AND DISCUSSION

We have examined the interplanetary causes of 10 large magnetic storms ( $Dst \leq -100$  nT) that occurred between the launch of ISEE 3 (August 16, 1978) and December 28, 1979 (500 days). Previously, Gonzalez and Tsurutani [1987] have shown that during this interval of study it was a necessary and sufficient criterion to have a dawn-dusk  $E > 5$  mV/m (approximately  $B_z \leq -10$  nT) with a duration  $\geq 3$  hours to generate the storms. Because of the required intensity of the southward magnetic fields the responsible interplanetary events would be expected to be associated with the high magnetic fields in the stream-stream interaction regions (sheaths) or driver gases. Nine of the 10 cases had such dependences, and the field events followed interplanetary shocks. The tenth event was somewhat of a surprise. It was associated not with a high-speed stream, but with a NCDE event.

In this study we have shown that four of the  $B_z$  events causing  $Dst$  to initially reach  $-100$  nT were associated with the plasma driver gas, with two having north-south (or vice versa) long-period magnetic oscillations, consistent with (but not proving) magnetic closure. One event had a south-north-south configuration, and the fourth event only a southward configuration. The other six storm events are due to an assorted variety of causes: one associated with shock intensification of "upstream" southward fields, possibly one or two with compressed kinky heliospheric current sheets, three or four with turbulent magnetic sheath fields, and one with possible field draping.

From the variety of causes of the responsible southward field events it is obvious that one cannot simply compare southward interplanetary magnetic fields at 1 AU and try to relate them to solar fields from the active "source" regions. The five events that are not related to driver gases are due to "upstream" quiet solar wind stream plasma that has been intensified (compressed) by the passage of collisionless shocks. This quiet solar wind plasma probably has an entirely different solar source [Hollweg, 1978; Marsch and Richter, 1984;

Freeman and Lopez, 1985]. Because of this finding, much of the prior work based on the assumption that storms were simply caused by outwardly convected magnetic fields from the solar active regions will have to be reevaluated.

One of the major goals of this study is to try to understand

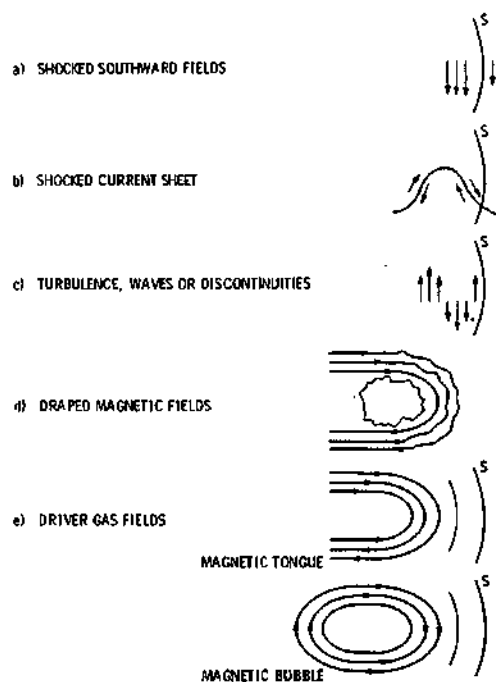


Fig. 13. A schematic of all the interplanetary magnetic field configurations which have led to geomagnetic storms in this study: (a) shocked southward interplanetary magnetic fields, (b) compressed kinky heliospheric current sheets, (c) compressed turbulence, waves, or discontinuities, (d) draped interplanetary magnetic fields, and (e) driver gas fields (magnetic bubbles and tongues).

the interplanetary and solar causes of major geomagnetic storms and to be able to determine whether it is possible to predict when they will occur and with what intensity. Clearly, at this stage it seems possible to understand this only for the cases where plasma drivers are responsible for the magnetic storms. For these specific cases we can test the model of simple outward propagation from the Sun without major field distortion [Pudovkin and Chertkov, 1976]. If we can demonstrate that there is a relationship between the driver gas  $B_z$  and the solar photospheric  $B_z$  (see Tang et al., submitted manuscript, 1988), there will be hope that quantitative predictions of the intensity of 40–60% of all major magnetic storms could be made, that is, if the duration of the southward IMF could be determined. If this cannot be done, then the percentage of predictability will decrease further.

The five interplanetary events which do not have any apparent relationship to driver gases can be understood if the entire time history of the slow solar wind plasma as it propagates from the Sun to 1 AU can be modeled. First, the solar sources of the slow stream plasma and fields will have to be identified. Then the evolution of the stream, as it interacts with other streams and the high-speed stream of interest, will have to be calculated. Computer simulations as described by Dryer and Steinolfson [1976] and Han et al. [1988] (see the particularly nice review by Pizzo [1985] and references therein) will be applicable. This task is quite difficult and should offer theoretical solar wind modelers a substantial challenge.

**Acknowledgments.** Data plots and PAAs were run out by L. W. Wigglesworth and L. Wagner. We wish to thank S. J. Bame for the use of the Los Alamos plasma data. Research described in this paper was carried out by the Jet Propulsion Laboratory, California Institute of Technology, under contract with the National Aeronautics and Space Administration.

The Editor thanks D. M. Rust and another referee for their assistance in evaluating this paper.

#### REFERENCES

- Abraham-Schrauner, B., Determination of magnetohydrodynamic shock normals, *J. Geophys. Res.*, **77**, 736, 1972.
- Akasofu, S.-I., Energy coupling between the solar wind and the magnetosphere, *Space Sci. Rev.*, **28**, 121, 1981.
- Akasofu, S.-I., C. Otmsted, E. J. Smith, B. Tsurutani, R. Okida, and D. N. Baker, Solar wind variations and geomagnetic storms: A study of individual storms based on high time resolution ISEE 3 data, *J. Geophys. Res.*, **90**, 325, 1985.
- Baker, D. N., R. D. Zwickl, S. J. Bame, E. W. Hones, Jr., B. T. Tsurutani, E. J. Smith, and S.-I. Akasofu, An ISEE 3 high time resolution study of interplanetary parameter correlations with magnetospheric activity, *J. Geophys. Res.*, **88**, 6230, 1983.
- Bame, S. J., J. R. Asbridge, H. E. Felthaus, J. P. Gore, H. L. Hawk, and J. Chaves, ISEE-C solar wind plasma experiment, *IEEE Trans. Geosci. Electron.*, **GE-16**, 160, 1978.
- Bame, S. J., J. R. Asbridge, W. C. Feldman, E. E. Fenimore, and J. T. Gosling, Solar wind heavy ions from flare-heated coronal plasma, *Sol. Phys.*, **62**, 179, 1979.
- Bavassano-Cattaneo, M. B., B. T. Tsurutani, E. J. Smith, and R. P. Lin, Subcritical and supercritical interplanetary shocks: Magnetic field and energetic particle observations, *J. Geophys. Res.*, **91**, 11,929, 1986.
- Belcher, J. W., and L. Davis, Jr., Large amplitude Alfvén waves in the interplanetary medium, *J. Geophys. Res.*, **76**, 3534, 1971.
- Burlaga, L. F., and K. W. Behannon, Magnetic Clouds: Voyager observations between 2 and 4 AU, *Sol. Phys.*, **81**, 181, 1982.
- Burlaga, L. F., K. W. Behannon, and L. W. Klein, Compound streams, magnetic clouds, and major geomagnetic storms, *J. Geophys. Res.*, **92**, 5725, 1987.
- Burton, R. K., R. L. McPherron, and C. T. Russell, An empirical relationship between interplanetary conditions and *Dst*, *J. Geophys. Res.*, **80**, 4204, 1975.
- Cane, H. V., The large-scale structure of flare-associated interplanetary studies, *J. Geophys. Res.*, **93**, 1, 1988.
- Dryer, M., and R. S. Steinolfson, MHD simulation of interplanetary disturbances generated by simulated velocity perturbations, *J. Geophys. Res.*, **81**, 5413, 1976.
- Dungey, J. W., Interplanetary magnetic field and the auroral zones, *Phys. Rev. Lett.*, **6**, 47, 1961.
- Frandsen, A. M. A., B. V. Connor, J. Van Amersfoort, and E. J. Smith, The ISEE-C vector helium magnetometer, *IEEE Trans. Geosci. Electron.*, **GE-16**, 195, 1978.
- Freeman, J. W., and R. E. Lopez, The cold solar wind, *J. Geophys. Res.*, **90**, 9885, 1985.
- Galvin, A. B., F. M. Ipavich, G. Gloeckler, D. Hovestadt, S. J. Bame, B. Klecker, M. Scholer, and B. T. Tsurutani, Solar wind iron charge states preceding a driver plasma, *J. Geophys. Res.*, **92**, 12,069, 1987.
- Gold, T., Magnetic storms, *Space Sci. Rev.*, **1**, 100, 1962.
- Gonzalez, W. D., and B. T. Tsurutani, Criteria of interplanetary parameters causing intense magnetic storms ( $Dst < -100$  nT), *Planet. Space Sci.*, **35**, 1101, 1987.
- Gosling, J. T., and D. J. McComas, Field line draping about fast coronal mass ejections: A source of strong out-of-the-ecliptic interplanetary magnetic fields, *Geophys. Res. Lett.*, **14**, 355, 1987.
- Gosling, J. T., A. J. Hundhausen, and S. J. Bame, Solar wind stream evolution at large heliospheric distances: Experimental demonstration and the test of a model, *J. Geophys. Res.*, **81**, 2111, 1976.
- Gosling, J. T., E. Hildner, J. R. Asbridge, S. J. Bame, and W. C. Feldman, Noncompressive density enhancements in the solar wind, *J. Geophys. Res.*, **82**, 5005, 1977.
- Gosling, J. T., D. N. Baker, S. J. Bame, W. C. Feldman, R. Zwickl, and E. J. Smith, Bidirectional solar wind electron heat flux events, *J. Geophys. Res.*, **92**, 8519, 1987.
- Han, S. M., S. T. Wu, and M. Dryer, A three-dimensional, time-dependent numerical modeling of super-sonic, super-Alfvénic MHD flow, *Comp. Fluids*, **16**, 82, 1988.
- Hirshberg, J., and D. S. Colburn, The interplanetary field and geomagnetic variations—A unified view, *Planet. Space Sci.*, **17**, 1183, 1969.
- Hollweg, J. V., Some physical processes in the solar wind, *Rev. Geophys.*, **16**, 689, 1978.
- Klein, L. W., and L. F. Burlaga, Interplanetary magnetic clouds at 1 AU, *J. Geophys. Res.*, **87**, 613, 1982.
- Landau, L. D., and E. M. Lifshitz, *Electrodynamics of Continuous Medium*, Pergamon, New York, 1960.
- Marsch, E., and A. K. Richter, Helios observational constraints on solar wind expansion, *J. Geophys. Res.*, **89**, 6599, 1984.
- Murayama, T., Coupling function between solar wind and the *Dst* index, in *Solar Wind-Magnetosphere Coupling*, edited by Y. Kamide, and J. A. Slavin, p. 119, Terra Scientific, Tokyo, Japan, 1986.
- Neugebauer, M., D. R. Clay, B. E. Goldstein, B. T. Tsurutani, and R. D. Zwickl, A reexamination of rotational and tangential discontinuities in the solar wind, *J. Geophys. Res.*, **89**, 5395, 1984.
- Patel, V. L., and M. J. Wiskerchen, Interplanetary field and plasma during initial phase of geomagnetic storms, *J. Geomagn. Geoelectr.*, **27**, 363, 1975.
- Pizzo, V. J., Interplanetary shocks on the large scale: A retrospective on the last decade's theoretical effort, in *Collisionless Shocks in the Heliosphere: Reviews of Current Research*, *Geophys. Monogr. Ser.*, vol. 35, edited by B. T. Tsurutani and R. G. Stone, p. 51, AGU, Washington, D. C., 1985.
- Pudovkin, M. I., and A. D. Chertkov, Magnetic field of the solar wind, *Sol. Phys.*, **50**, 213, 1976.
- Pudovkin, M. I., and S. A. Zaitseva, Comment on "Magnetic Field on the Sun and the North-South Component of Transient Variation of the Interplanetary Magnetic Field at 1 AU" by F. Tang et al., *J. Geophys. Res.*, **91**, 13,765, 1986.
- Pudovkin, M. I., S. A. Zaitseva, and E. E. Benevolskaya, The structure and parameters of flare streams, *J. Geophys. Res.*, **84**, 6649, 1979.
- Rostoker, G., and C. G. Fälthammar, Relationship between changes in the interplanetary magnetic field and variations in the magnetic field at the Earth's surface, *J. Geophys. Res.*, **72**, 5853, 1967.
- Smith, E. J., Identification of interplanetary tangential and rotational discontinuities, *J. Geophys. Res.*, **78**, 2054, 1973.
- Smith, E. J., Solar wind magnetic field observations, *Solar Wind Four*, *Tech. Rep. MPAE-W-100-81-31*, edited by H. Rosenbauer, p. 96, Max-Planck-Institut für Aeronomie, Katlenburg-Lindau, Federal Republic of Germany, 1981.
- Smith, E. J., and B. T. Tsurutani, Magnetosheath lion roars, *J. Geophys. Res.*, **81**, 2261, 1976.

- Smith, E. J., and J. H. Wolfe, Observations of interaction regions and corotating shocks, *Geophys. Res. Lett.*, **3**, 137, 1976.
- Smith, E. J., B. T. Tsurutani, and R. L. Rosenberg, Observations of the interplanetary sector structure up to heliographic latitudes of  $16^\circ$ : Pioneer 11, *J. Geophys. Res.*, **83**, 717, 1978.
- Smith, E. J., J. A. Slavin, R. D. Zwickl, and S. J. Bame, Shocks and storm sudden commencements, in *Solar Wind Magnetosphere Coupling*, edited by Y. Kamide and J. A. Slavin, D. Reidel, Hingham, Mass., 1986.
- Stone, R. G., and B. T. Tsurutani (Eds.), *Collisionless Shocks in the Heliosphere: A Tutorial Review*, *Geophys. Monogr. Ser.*, vol. 34, AGU, Washington, D. C., 1985.
- Tang, F., S.-I. Akasofu, E. J. Smith, and B. T. Tsurutani, Magnetic fields on the Sun and the north-south component of transient variations of the interplanetary magnetic field at 1 AU, *J. Geophys. Res.*, **90**, 2703, 1985.
- Tang, F., S.-I. Akasofu, E. J. Smith, and B. T. Tsurutani, Reply, *J. Geophys. Res.*, **91**, 13,769, 1986.
- Tidman, D. A., and N. A. Krall, *Shock Waves in Collisionless Plasmas*, John Wiley, New York, 1971.
- Tsurutani, B. T., and W. D. Gonzalez, The cause of high-intensity long-duration continuous AE activity (HILDCAAs): Interplanetary Alfvén wave trains, *Planet. Space Sci.*, **35**, 405, 1987.
- Tsurutani, B. T., and R. P. Lin, Acceleration of  $>47$ -keV ions and  $>2$ -keV electrons by interplanetary shocks at 1 AU, *J. Geophys. Res.*, **90**, 1, 1985.
- Tsurutani, B. T., C. T. Russell, J. H. King, R. D. Zwickl, and R. P. Lin, A kinky heliospheric current sheet: Cause of CDAW 6 substorms, *Geophys. Res. Lett.*, **11**, 339, 1984.
- Tsurutani, B. T., J. A. Slavin, Y. Kamide, R. D. Zwickl, J. H. King, and C. T. Russell, Coupling between the solar wind and the magnetosphere: CDAW 6, *J. Geophys. Res.*, **90**, 1191, 1985.
- Unti, T. W., G. Atkinson, C. S. Wu, and M. Neugebauer, Dissipation mechanisms in a pair of solar wind discontinuities, *J. Geophys. Res.*, **77**, 2250, 1972.
- Zwickl, R. D., J. R. Asbridge, S. J. Bame, W. C. Feldman, J. T. Gosling, and E. J. Smith, Plasma properties of driver gas following interplanetary shocks observed by ISEE-3, Solar Wind Five, *NASA Conf. Publ.*, CP-2280, 711, 1983.
- Zwickl, R. D., L. F. Bargatze, D. N. Baker, C. R. Clauer, and R. L. McPherron, An evaluation of the total magnetospheric energy output parameter,  $U_T$ , in *Magnetotail Physics*, edited by A. T. Y. Lui, p. 155, Johns Hopkins Press, Baltimore, Md., 1987.
- S.-I. Akasofu, Geophysical Institute, University of Alaska, Fairbanks, AK 99775.
- W. D. Gonzalez, E. J. Smith, and B. T. Tsurutani, Jet Propulsion Laboratory, California Institute of Technology, Pasadena, CA 91109.
- F. Tang, California Institute of Technology, Pasadena, CA 91125.

(Received November 19, 1987;  
revised March 24, 1988;  
accepted March 24, 1988.)